J Ther Eng, Vol. 10, No. 1, pp. 142−152, January, 2024

Journal of Thermal Engineering
Web page info: https://jten.yildiz.edu.tr
DOI: 10.18186/thermal.1429444

Research Article

Numerical investigation of forced convection flow of a complex Bingham–Papanastasiou fluid between two concentric cylin-ders with a wavy inner wall

Benhanifia KADA[1,*], Fares REDOUANE[2], Lakhdar RAHMANI[1], Naveen Kumar GUPTA[3], Mebarki BRAHIM[1], Hitesh PANCHAL[4], Saeed NAZARI[5], Abhinav KUMAR[6], Anand PATEL[7]

[1]*Laboratory of Energy in Arid Region (ENERGARID), Faculty of Science and Technology, University of Tahri Mohamed Bechar, P.O. Box 417, Bechar 08000, Algeria*

[2]*LGIDD, Department of physics, Faculty of Science and Technology, Relizane university, 48000, Relizane, Algeria*
[3]*Department of Mechanical Engineering, GLA University, Mathura, 281406, India*
[4]*Department of Mechanical Engineering, Government Engineering College Patan, Gujarat, 636011, India.*
[5]*Department of Mechanical Engineering, Ural Federal University, 620002, Russia*
[6]*Department of Medical Instruments Engineering Techniques, Al-farahidi University, Baghdad, 00965, Iraq*
[7]*Department of Mechanical Engineering, LDRP Institute of Engineering and Technology, Gandhinagar, Gujarat, 382016, India*

ARTICLE INFO

Article history
Received: 17 July 2023
Accepted: 29 August 2023

Keywords:
Forced Convection; Complex Bingham –Papanastasiou Fluid; Concentric Cylinder; Finite Element Method

ABSTRACT

This research presents a numerical investigation of the flow field and heat transfer of a Visco-plastic fluid, The Bingham-Papanastasiou model is used to examine the flow field and forced convection heat transfer of a Viscoplastic fluid between two concentric cylinders with a wavy inner surface. By focusing on this particular configuration (wavy inner cylinder shape), where the inner surface exhibits as the hot wall while the outer surface is considered as the cold wall. This investigation is numerically achieved by using the Comsol Multiphysics, which is based on the finite-volume method, employing Galerkin's method for solving the governing equations. The parameters studied in this research are expressed with the following values: r/R=1/3, Reynolds number (Re=1, 10, 50), and undulation number (n_u=0, 6, 12, 24). Increasing the inertia parameter results in a higher intensity of thermal buoyancy, positively influencing heat transfer, particularly at Re=50. Furthermore, the acceleration of flow within the investigated space improves the hydrodynamic behavior, facilitating the exchange of thermal energy between the hot and cold walls. Additionally, it has been discovered that an undulating shape with a specific number of undulations (n_u=6) maximizes hydrothermal performance within the investigated volume. The presence of these undulations enhances fluid mixing and disrupts the formation of stagnant regions ,which leading to improved heat transfer.

Cite this article as: Kada B, Redouane F, Rahmani L, Gupta NK, Brahim M, Panchal H, Nazari S, Kumar A, Patel A. Numerical investigation of forced convection flow of a complex Bingham–Papanastasiou fluid between two concentric cylin-ders with a wavy inner wall. J Ther Eng 2024;10(1):142−152.

***Corresponding author.**
*E-mail address: benhanifia.kada@univ-bechar.dz

This paper was recommended for publication in revised form by Ahmet Selim Dalkılıç

INTRODUCTION

Thermal exchange of a non-Newtonian fluid is required widely in many engineering applications, such as in solar collectors and thermal storage systems, polymer engineering, cooling of electronic devices, food processing, etc. This application is mostly directed at cylindrical heat devices. The optimization of the performance of these devices requires extensive knowledge of the thermal behavior and flow pattern mechanism [1–3]. Recently many researchers have excellent attention to the problem of viscoplastic fluid flow because of its wide application in petroleum production, chemical process industries and construction engineering, and commercial applications [4–6]. The behavior of the fluid and its physicochemical characteristics, and the geometrical design of the heat exchanger, are considered the most important factors affecting the thermal system process.

The circular annulus shape is one of the industry's most existing geometries. It is widely applied by many researchers in various theoretical, experimental and numerical simulation studies [6–14]. Numerous researchers considered the flow and thermal behavior inside a coaxial cylinder. In contrast, most researchers have referred to the circular shape geometry as the standard configuration shape [15,16]. Some researchers focused on the investigation of non-Newtonian fluids between coaxial cylinders such as [11,16–20]. A few studies address the viscoplastic fluid category. For instance, [15] conducted a numerical investigation of viscoplastic fluid flow based on the Carreau fluid model within concentric cylinders. Their findings display that the shear thinning effect reduces the friction coefficient on the rotating cylinder and raises the thermal transfer. Also, an oscillatory flow was observed because of the reduction in the apparent viscosity, notably in centrifugal forced convection.

Some rare studies have investigated the flow of these viscoplastic fluids (yield stress fluid), especially the flow of these fluids inside the space between coaxial cylinders. One of these studies is [16], who conducted a numerical study focused on the natural convection of a yield stress fluid between two cylinders. They analyzed the effect of rheological and geometrical parameters on thermal behavior. They found that the thermal flow decreased due to the increase in the yield stress parameter. Nazari et al. [17] investigate the mixed flow and heat transfer of non-Newtonian water/Al_2O_3 nanofluid inside a two-dimensional porous cavity. They studied the hydrodynamic flow and heat transfer in cavity with hot and cold lid-driven motion in two different cases. Their Results reveals that variations of nanoparticles volume fraction of cooling nanofluid and penetrability of fluid direction (Darcy number) are important factors which influence the streamline behavior. Khan et al. [18] investigated the free convection of Casson fluid inside a square cavity with Y-shaped fin at the bottom surface. They showed that the presence of Y-shaped fin enhanced the heat transfer rate along the bottom surface. Farooq et al. [19] examined the impact of an external magnetic field on the hydrothermal aspects of natural convection of a power-law non-Newtonian nanofluid inside a baffled U-shape enclosure. They concluded that the effect of n and Ha on the heat transfer is high when Ha (Hartman number) is smaller than 30. For Ha<30, there is a threshold value of nanoparticle after which the rise of n (the flow behavior index) enhancement heat transfer, which is 5% for (AR : the aspect ratio of cold baffles)AR=0.4 and 7% for AR=0.6. Raihan et al. [20] experimentally studied the flow of five types of non-Newtonian fluids with distinct rheological properties and water through a planar single-cavity microchannel. Their results showed that fluid inertia induces circulations in the expansion flow of water, which is trivially impacted by the confinement as the expansion flow circulations are merely restricted from growing at the contraction walls without showing any other significant event or instability. Bisht et al. [21] examined the flow of non-Newtonian fluid inside the lid-driven cavity with obstacle(s). The behavior of the fluid is illustrated by the Ostwald-de Waele or power-law model. They revealed that Reynolds number (with respect to lid-dimension), obstacle size, power-law index, and shape of the obstacle on the flow characteristics and vortex formation can be positive effect on heat transfer of the problem.

Based on the previous literature studies, there appear to have been no reports on the analysis of forced convection of Bingham–Papanastasiou fluids in annular spaces between concentric cylinders. Therefore, this work aims to conduct complete numerical research of the problem, specifically focusing on viscoplastic fluids' hydrodynamic flow and thermal transfer properties in various operational settings. The inertia effect on the thermo-hydrodynamic structure is considered for a range of Reynolds numbers Re [1, 10, 50] and geometric configurations, with the first case assuming a standard inner-cylinder design and the others introducing a new wavy inner-cylinder shape with a range of undulation numbers n. [6, 12, 24]. This modification can interpret the system's flow pattern and thermal behavior.

PHYSICAL MODEL

Figure 1 illustrates a diagram of the two-dimensional concentric cylinders. In this study, we represent two different geometry configurations. Case 1 considers a simple concentric cylinder schematic, while Case 2 considers a wavy inner cylinder, and the outer one is a circular shape.

The wavy shape varies from 0 to 24 in several undulations. For all these cases, we assume the inner wall to rotate, which is assumed to be the hotter cylinder under constant temperature, Th. In contrast, the outer is assumed to be the cold part under constant temperature, Tc.

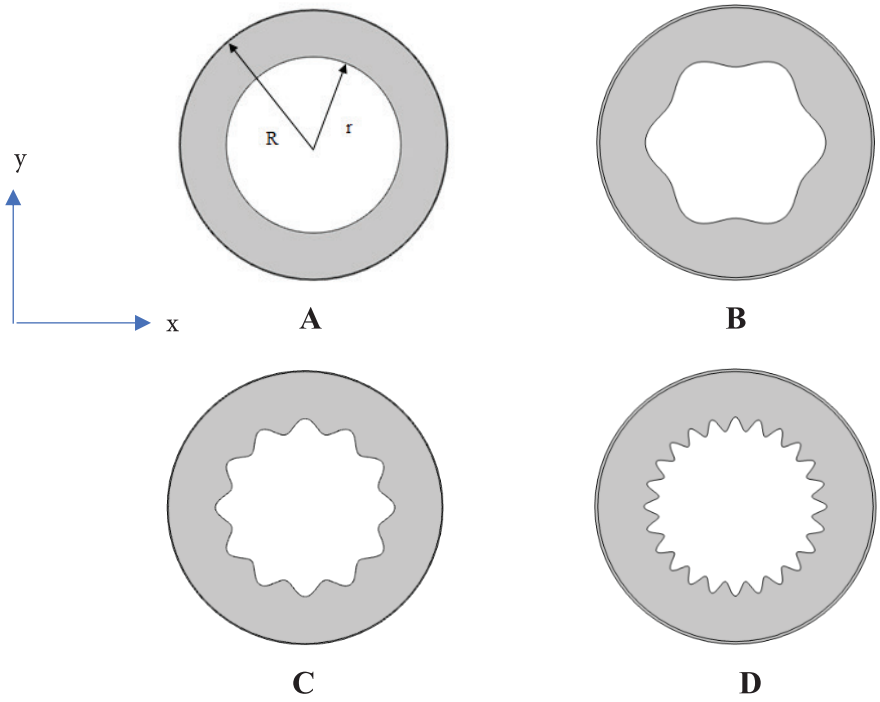

Figure 1. A physical model of the studied annular space.

MATHEMATICAL DESCRIPTION

The numerical simulation of the thermal behavior for the flow of a viscoplastic (Bingham-Papanastasiou model) fluid inside a coaxial cylinder performed. The configuration consists of a rotating inner cylinder under constant hot temperature (Th) and a fixed outer wall under constant cold temperature Tc. Figure 2 shows the numerical implementation of the simulations done with the Comsol Multiphysics code. It solves the momentum and energy equations (7–10) using the finite element method and Galerkin's discretization on an unstructured mesh. In the discretization of the computational domain, a tetrahedral mesh is introduced, and it is particularly suitable for representing the geometrical domain due to its high adaptability to curved surfaces. The main reason for unstructured interleaving is that it provides a more accurate solution to the governing equations around the cylinder (especially the inner cylinder). The solution is assumed to converge when the relative error values of the velocity components and the temperature field are less than 10^{-6}.

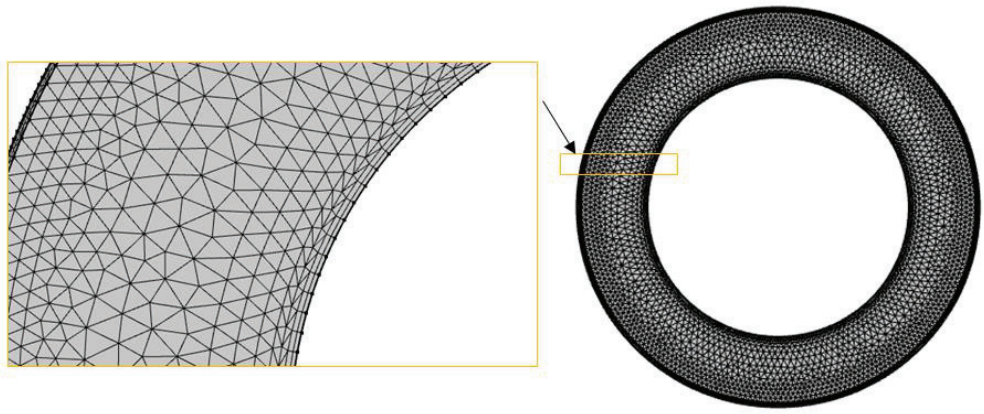

Figure 2. Tetrahedral mesh structure.

Mesh Analysis Test

A mesh analysis test is conducted under the condition of two circular coaxial cylinder shapes for an inertia value Re =1 and the Bingham-Papanastasiou fluid model .Here, we verify the grid's adequacy by testing it with four different mesh types (using the software's defaults), as shown in Table 1. It ensures that our results are grid-independent. As seen, for both average Nusselt number Nu results, the maximum value of Nu is reached and fixed at the finer mesh, and we chose this size due to its suitability from the accuracy computation viewpoint.

Nu = ……

Table 1. Grid test

Mesh type	Mesh element	Nu average	CPU time
Normal	3838	0.4540	16 **s**
Fine	4416	0.45554	17 **s**
finer	**7570**	**0.46052**	**41 s**
Extra mesh	18812	0.4602	35 **s**

The governing equations of continuity, momentum, and energy equations, and the system solved under these hypotheses :

- **The working fluid is a non Newtonian fluid Viscoplastic model**
- **2-D Steady–state flow**
- **The regime is supposed to be laminar**

and these equations are given as follows:

Dimensional equations:

Continuity equation:

$$\frac{\partial U}{\partial X}+\frac{\partial V}{\partial Y}=0 \tag{1}$$

Momentum equation:

$$\rho\left(\mathrm{U}\frac{\partial \mathrm{U}}{\partial \mathrm{X}}+\mathrm{V}\frac{\partial \mathrm{U}}{\partial \mathrm{Y}}\right)=-\frac{\partial \mathrm{P}}{\partial \mathrm{X}}+\left[\frac{\partial}{\partial \mathrm{X}}\left(2\left(\mu_p+\frac{\tau}{\dot{\gamma}}\exp\left(1-m\dot{\gamma}\right)\right)\frac{\partial \mathrm{U}}{\partial \mathrm{X}}\right)+\frac{\partial}{\partial \mathrm{X}}\left(\left(\mu_p+\frac{\tau}{\dot{\gamma}}\exp\left(1-m\gamma\right)\right)\left(\frac{\partial \mathrm{U}}{\partial \mathrm{Y}}+\frac{\partial \mathrm{V}}{\partial \mathrm{X}}\right)\right)\right] \tag{2}$$

$$\rho\left(\mathrm{U}\frac{\partial \mathrm{V}}{\partial \mathrm{X}}+\mathrm{V}\frac{\partial \mathrm{V}}{\partial \mathrm{Y}}\right)=-\frac{\partial \mathrm{P}}{\partial \mathrm{Y}}+\left[\frac{\partial}{\partial \mathrm{Y}}\left(2\left(\mu_p+\frac{\tau}{\dot{\gamma}}\exp\left(1-m\dot{\gamma}\right)\right)\frac{\partial \mathrm{V}}{\partial Y}\right)+\frac{\partial}{\partial \mathrm{Y}}\left(\left(\mu_p+\frac{\tau}{\dot{\gamma}}\exp\left(1-m\dot{\gamma}\right)\right)\left(\frac{\partial \mathrm{U}}{\partial \mathrm{Y}}+\frac{\partial \mathrm{V}}{\partial \mathrm{X}}\right)\right)\right] \tag{3}$$

Energy equation:

$$U\frac{\partial T}{\partial X}+V\frac{\partial T}{\partial Y}=\alpha\left(\frac{\partial^2 T}{\partial X^2}+\frac{\partial^2 T}{\partial Y^2}\right) \tag{4}$$

Papanastasiou (1987) (23) presented an exponential regularization of the stress equation to avoid discontinuities between a yield-stressed material's yielded and non- . Based on this model, equation (5) is expressed as (24):

$$\mu=\mu_p+\frac{\tau}{\gamma\&}\exp\left(1-m\,\gamma\&\right) \tag{5}$$

where μ_p represents the plastic viscosity, m is called a regularization parameter or the stress growth exponent, $\dot{\gamma}$ is the shear rate, and τ is the shear stress.

Dimensionless parameters

$$X^*=\frac{X}{D}\qquad Y^*=\frac{Y}{D}\qquad U^*=\frac{U}{\pi ND}\qquad V^*=\frac{V}{\pi ND}$$
$$P^*=\frac{P}{\rho(\pi ND)^2}\qquad ;\qquad \pi ND^{-}\gamma\qquad T^*=\frac{T-T_c}{T_h-T_c} \tag{6}$$

Dimensionless equations:

Continuity equation

$$\frac{\partial U^*}{\partial X^*}+\frac{\partial V^*}{\partial Y^*}=0 \tag{7}$$

Momentum equation

$$\mathrm{U}^*\frac{\partial \mathrm{U}^*}{\partial \mathrm{X}^*}+\mathrm{V}\frac{\partial \mathrm{U}^*}{\partial \mathrm{Y}^*}=-\frac{\partial \mathrm{P}^*}{\partial \mathrm{X}^*}+\frac{1}{\mathrm{Re}}\left[\begin{array}{l}\frac{\partial}{\partial \mathrm{X}^*}\left(2\left(1+\frac{Bn}{\gamma^*}\left(1-\exp\left(-M\gamma^*\right)\right)\right)\frac{\partial \mathrm{U}^*}{\partial \mathrm{X}^*}\right)\\+\frac{\partial}{\partial \mathrm{X}^*}\left(\left(1+\frac{Bn}{\gamma^*}\left(1-\exp\left(-M\gamma^*\right)\right)\right)\left(\frac{\partial \mathrm{U}^*}{\partial \mathrm{Y}^*}+\frac{\partial \mathrm{V}^*}{\partial \mathrm{X}^*}\right)\right)\end{array}\right] \tag{8}$$

$$\mathrm{U}^*\frac{\partial \mathrm{V}^*}{\partial \mathrm{X}^*}+\mathrm{V}\frac{\partial \mathrm{V}^*}{\partial \mathrm{Y}^*}=-\frac{\partial \mathrm{P}^*}{\partial \mathrm{Y}^*}+\frac{1}{\mathrm{Re}}\left[\begin{array}{l}\frac{\partial}{\partial \mathrm{Y}^*}\left(2\left(1+\frac{Bn}{\gamma^*}\left(1-\exp\left(-M\gamma^*\right)\right)\right)\frac{\partial \mathrm{V}^*}{\partial \mathrm{X}^*}\right)\\+\frac{\partial}{\partial \mathrm{Y}^*}\left(\left(1+\frac{Bn}{\gamma^*}\left(1-\exp\left(-M\gamma^*\right)\right)\right)\left(\frac{\partial \mathrm{U}^*}{\partial \mathrm{Y}^*}+\frac{\partial \mathrm{V}^*}{\partial \mathrm{X}^*}\right)\right)\end{array}\right] \tag{9}$$

Energy equation

$$U^*\frac{\partial T^*}{\partial X^*}+V^*\frac{\partial T^*}{\partial Y^*}=\frac{1}{Re\ Pr}\left(\left(\frac{\partial^2 T^*}{\partial X^{*2}}\right)+\left(\frac{\partial^2 T^*}{\partial Y^{*2}}\right)\right) \tag{10}$$

The dimensionless viscosity of the Bingham-Papanastasiou fluid is written as the following equation (24):

$$\mu^*=1+\frac{Bn}{\gamma^*}\left(1-\exp\left(-M\gamma^*\right)\right) \tag{11}$$

Dimensionless parameters:

Bingham number (24)

$$Bn=\frac{\tau D}{\mu N} \tag{12}$$

D : diameter of the outer cylinder μ : dynamic viscosity

N : rotation speed τ : stress tensor

Reynolds Number (6)

$$\mathrm{Re}=\frac{\rho ND^2}{\mu} \tag{13}$$

Local Nusselt number (25)

$$Nu_L = \frac{\partial T^*}{\partial n} \tag{14}$$

Average Nusselt number (25)

$$\overline{Nu} = \frac{1}{A}\int \frac{\partial T^*}{\partial n} \tag{15}$$

The streamlines results shown in the result are partly extracted from the stream function (ψ) that is defined from the components of velocity U and V, and their relations are expressed by :

$$U = \frac{\partial \psi}{\partial Y} \qquad V = -\frac{\partial \psi}{\partial X} \tag{16}$$

Validation

For verification and confirmation of the fiability and performance of the calculation of code used, we refer to the studies of (26)] and (22)].

First, we compare our simulation result (shown in Figure 3) favorably to an analytic solution of a viscoplastic fluid flow (Bingham model) between two cylinders, where the outer cylinder is the rotating part. It is done by referring to the work of (Marouche and Boisson 2002). We used all geometrical and rheological parameters for performing this study (a working fluid with the characterization (μ = 0.1, τ = 0.1 with inertia value (Re=13.8)).

For the second comparison, the streamlined visualization of (Masoumi et al. 2019) has been simulated in the same geometrical and rheological conditions (D/d = 2, Ra = 105, and the working fluid is the Bingham fluid with rheology parameter (Y = 0.02,0.03, 0.048). Figure 4 illustrates the streamlined result of the study (Masoumi et al. 2019) with (Rayleigh number) Ra = 10^5 for different yield stress parameters (Y = 0.02, 0.03, 0.08) and it is a comparison with our findings.

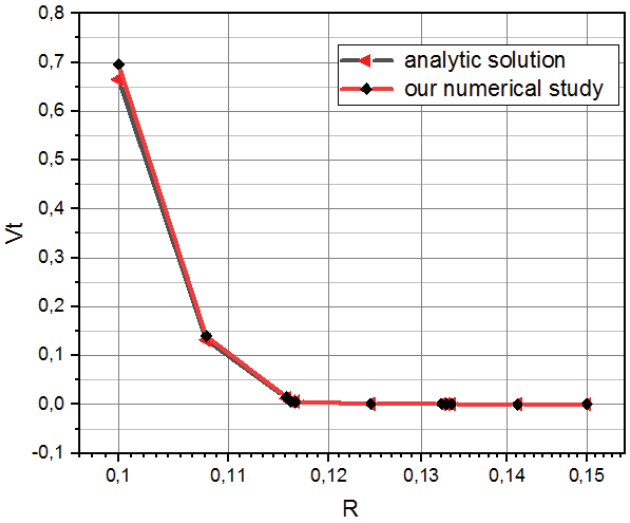

Figure 3. Tangential velocity values of the analytic solution of Marouche and Boisson 2002 (26) compared with our numerical study.

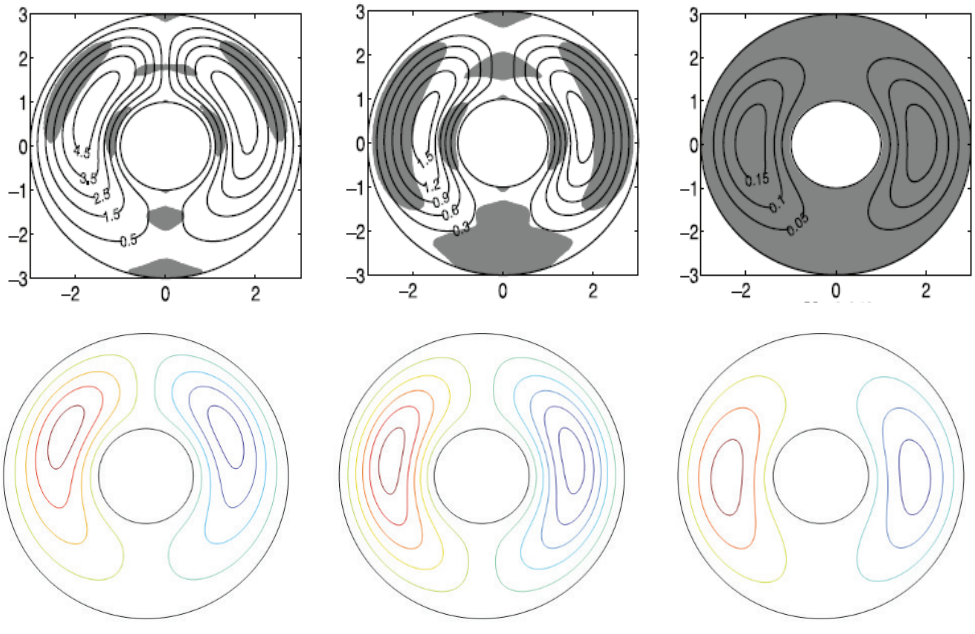

Figure 4. Comparison of streamlined contours with Ra = 105 with Masoumi et al. 2019 [16].

The results are incredibly similar to the previous numerical results of Marouche and Boisson (2002) (26)] and Masoumi 2019 (22)].

RESULTS AND DISCUSSION

In this part, we investigate the thermal hydro-thermal structure of the fluid flow inside the space between the coaxial cylinders. This investigation is visualized using the flow pattern (velocity) streamlines, isotherms, and the average Nusselt number.

Inertia Effect

This section presents the effect of inertia parameters on the inside coaxial cylinder. Figure 5 illustrates the velocity contours distribution between the concentric cylinders for different Reynolds numbers Re = 1, 10, 50.

A regularity (uniform distribution) of velocity distribution from the inner to the outer cylinder along the horizontal and the vertical axes is observed. However, with low inertia value of Re = 1, the velocity magnitude can reach a maximum of 0.57 in addition with the inertia value Re = 10 the velocity become 5.7. In contrast, for high inertia of Re=50, it can reach a value of 28.5. we can note that the increase in inertia parameter lead to improve the flow between concentric cylinders .

Figure 6 Show the velocity distribution along the inner/outer cylinder space. The results indicate that varying the undulation number has a positive effect on the hydrodynamic characterization of the flow, at the initial edge of the inner cylinder, it is evident that the velocity of the configuration with an undulation number of n_u = 6 is lower, measuring 0.55, in comparison to the velocity of the other configuration, which is 0.65. However, as we progress further along the surface, the configuration with an undulation number of n=6 outperforms all other configurations in terms of velocity values. This superiority is maintained for approximately 40% of the remaining surface. This configuration leads to a significant acceleration of the tangential flow within the concentric cylinder space and It is noteworthy that the wavy surface with n_u = 6 undulations exhibits the highest efficiency compared to all other configurations.

Average Nusselt Number

Figure 7 presents the average value of the Nusselt number for different inertia values Re = (1, 10, 50). An increase in the heat transfer rate with the inertia value is observed. We note that the rise in the Reynolds number encourages the increase in heat transfer and, therefore, the average Nusselt number. As can be seen from the diagram in Figure 7, the trend of increasing Nusselt number with increasing Re number is almost linear. Therefore, in this case, it can

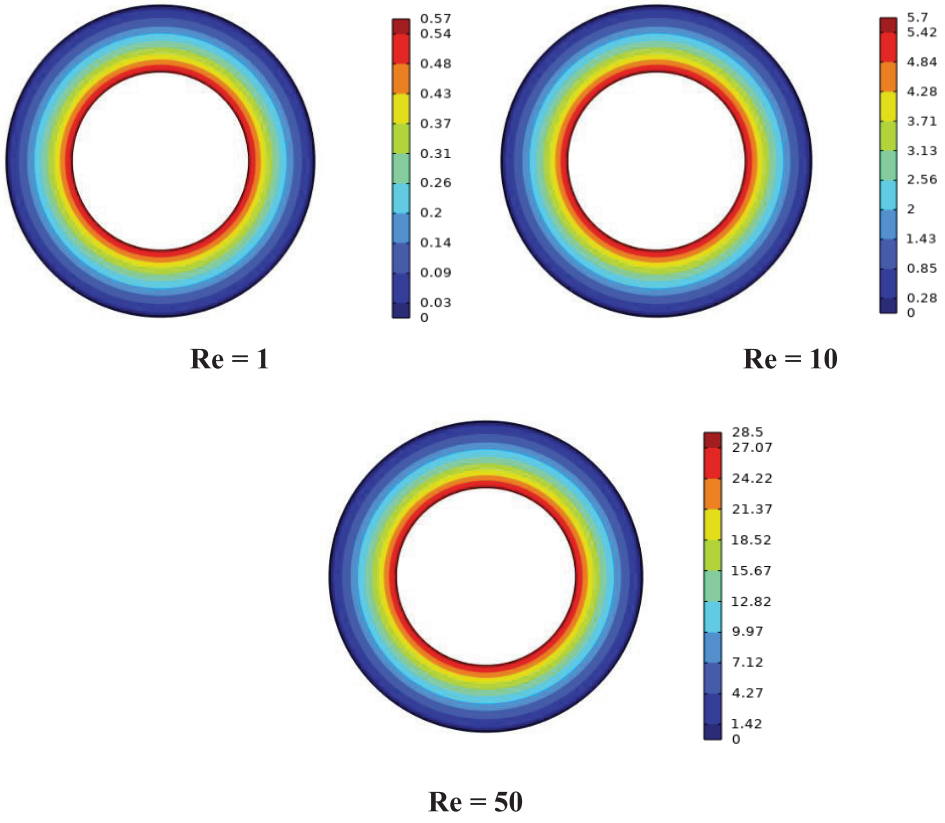

Figure 5. Velocity distribution inside annular space for different inertia values (Re = 1, 10, 50)

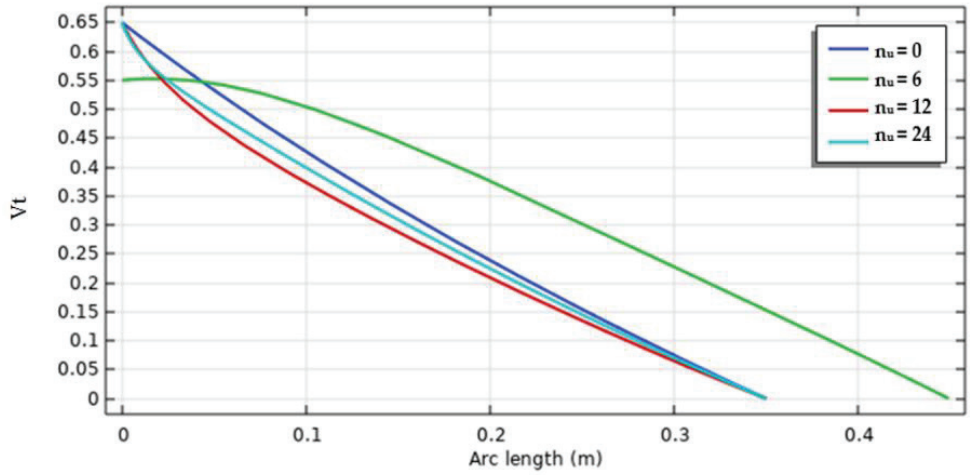

Figure 6. Tangential velocity values for different undulations numbers.

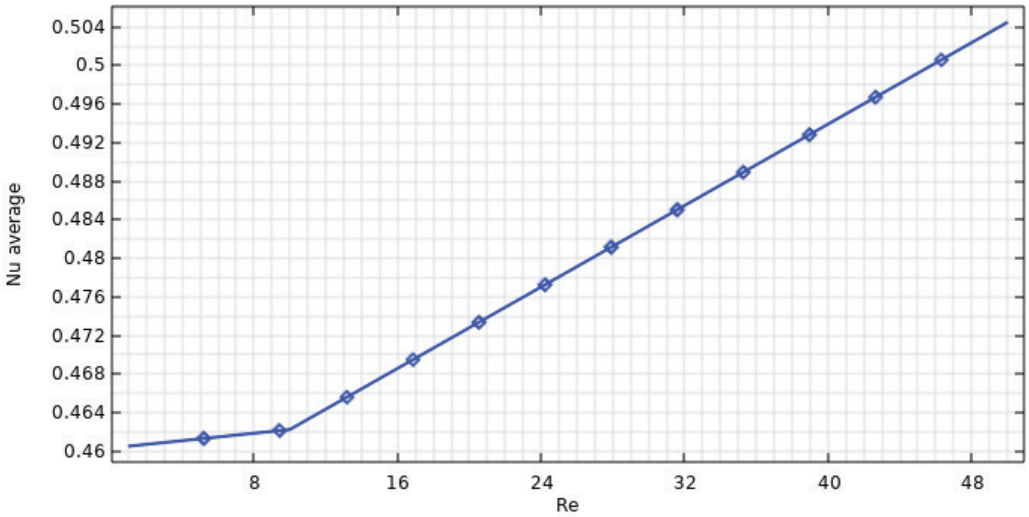

Figure 7. Average Nusselt number as function as Reynolds numbers.

be concluded that convection heat transfer has a linear relationship with Re number.

Temperature Contours

The isotherm patterns in Figures 8 (ABCD) reveals the effects of the amplitudes of the inner wavy cylinder (n: undulation numbers) and the inertia values (Re: Reynolds numbers) on the thermal flow structure.

For the first case of the standard shape of coaxial cylinders, we notice that the thermal flow inside the annulus is weak and is limited only near the wall for a low inertia value Re = 1,10. The isotherm contours are distributed regularly from the inner wall toward the external wall. As the inertia value increases (Re = 50), this rise in Reynolds number leads to a significant change in the thermal behavior accompanied by an expansion of the heated zone comparatively with the previous inertia values.

However, in the other wavy inner cylinder surface cases, the same remark of the previous standard shape regularity in the heat line distribution for low inertia value Re = 1,10 is in order. Nevertheless, an introduction of undulations in the inner cylinder surface significantly influences the thermal behavior with the acceleration of heat transfer and amplification of the heated zone. This geometrical design is more efficient than the inner cylinder's standard shape.

Streamlines

The streamline contours determine the flow path within the space, from which it is possible to identify the regions in which the heat transfer is strong or weak. The streamlines

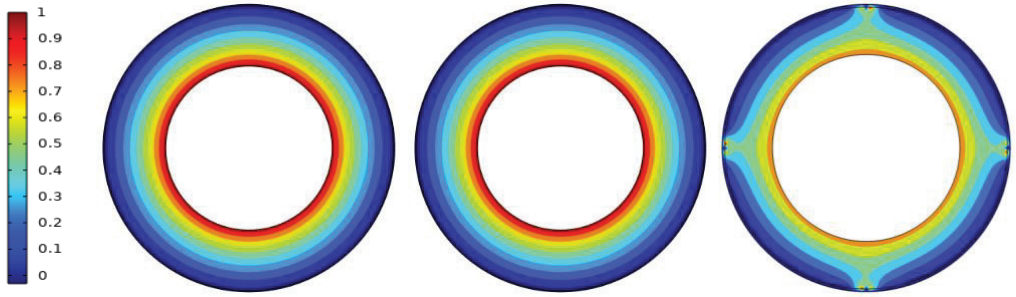

Re = 1 **Re = 10** **Re = 50**

A: Standard shape of coaxial cylinders n_u =0.

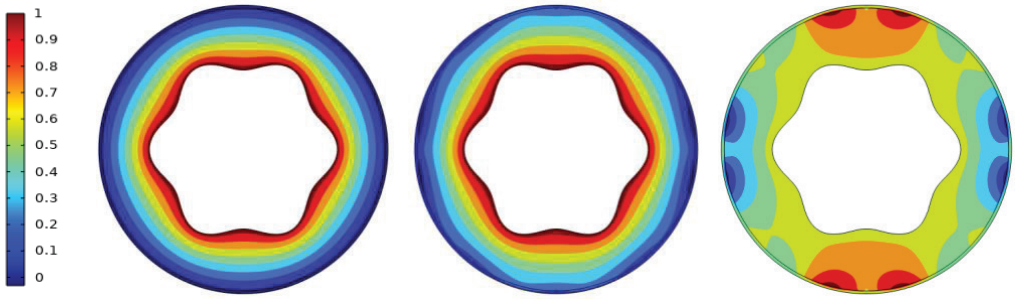

Re = 1 **Re = 10** **Re = 50**

B: wavy inner wall of coaxial cylinders n_u =6.

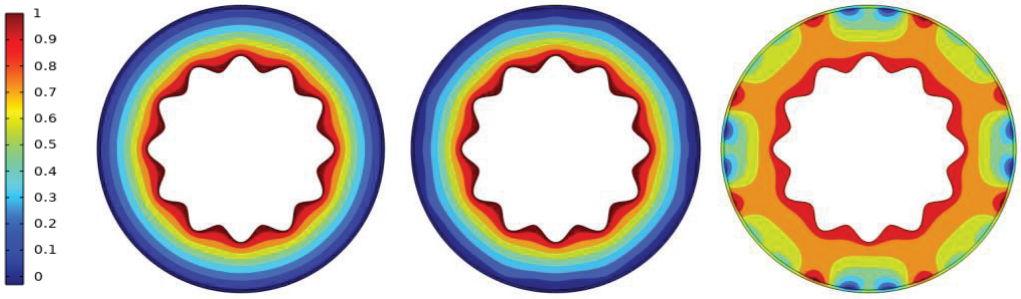

Re = 1 **Re = 10** **Re = 50**

C: Wavy inner wall of coaxial cylinders n_u =12.

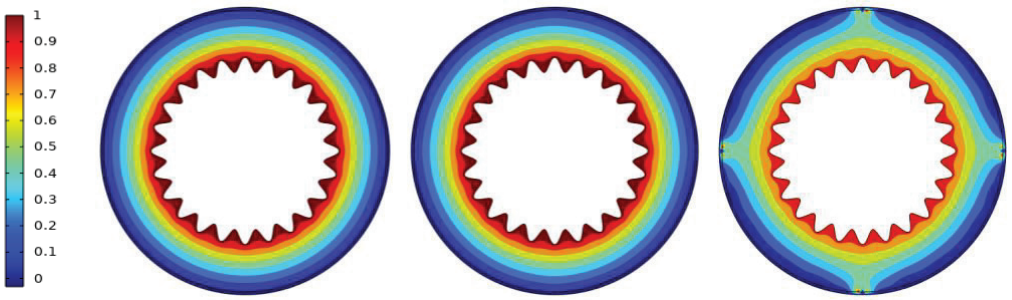

Re = 1 **Re = 10** **Re = 50**

D: Wavy inner wall of coaxial cylinders n_u =24.

Figure 8. Isothermal contours for different geometry designs of inner cylinders.

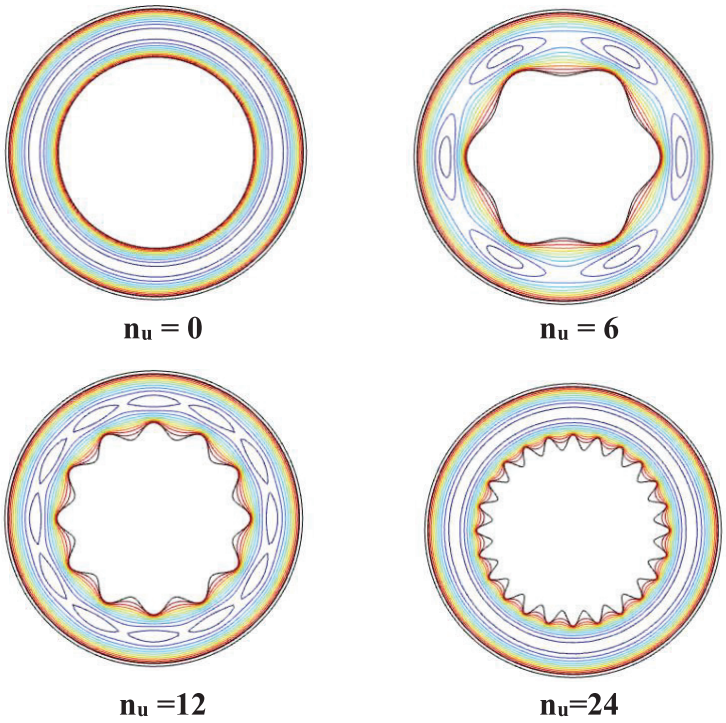

Figure 9. Streamlines distribution inside the gap annulus.

give detailed visualization of flow fields and particle trajectories to determine moving/stagnant regions.

Figure 9 presents the streamlined distribution along the space between cylinders, whereas it is done for different numbers of undulations (n_u = 0, 6, 12, 24)

For the standard shape of the inner cylinder (n=0), the streamlined contours exhibit regular parallel eddies. The vortices are being created with a change in shape, with the undulation numbers n_u = 6 and 12 developing along the annulus gap. These vortices increase the heat transfer rates between the two cylinders.

The existence of the inner cylinders as flow obstructions causes the appearance of these vortices, with the eddy being pushed from the wavy surface of the inner cylinder by the centrifugal force and propagated to the number of cells (six vortex cells for case n= 6; eleven vortex cells for case n_u = 24). For the final case of undulation number n= 48, a disappearance of this cell has been observed.

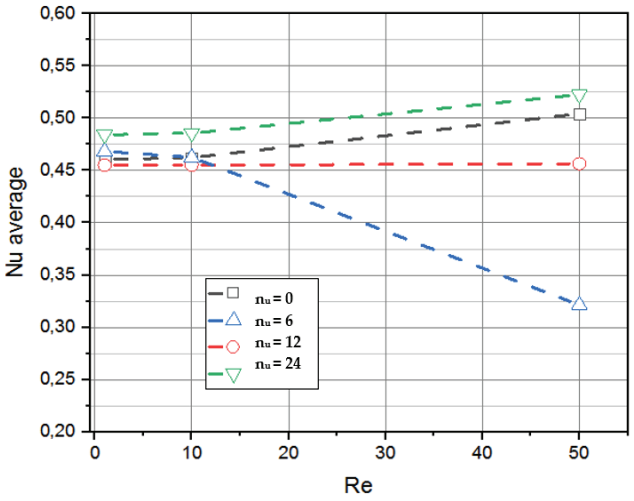

Figure 10. Average Nusselt number versus different geometry configurations along the inertia variation (Re = 1, 10, 50).

Average Nusselt Number

Figure 10 presents the average value of the Nusselt number for different geometry configurations of the inner cylinder by varying the undulation number (n_u = 0, 6, 12, 24). The rate of the thermal exchange is found to be the biggest for the case of an inner cylinder with an undulations number of n_u = 24.

For n_u = 0 and n_u = 24, with the increase of Re number, the average Nusselt value of the change increases almost. For n_u = 12, the average Nusselt number does not change with increasing Re number. However for n_u = 6, in the range of Reynolds numbers Re < 10, the average Nusselt does not affected by Reynolds variation and become constatnt at the value of 0.45, on the other hand espicially for Reynolds numbers Re= 50, the average Nusselt value decreases dramatically heat transfer rate n_u= 0.33.

The wavy cylinder shape with an undulation number of nu=24 outperformed other cases in terms of thermal efficiency, exhibiting significantly higher heat transfer rates (Nusselt value). Its unique configuration led to notable improvements in heat transfer capabilities.

CONCLUSION

This study was carried out numerically to examine a set of related parameters for heat transfer and hydrodynamic behavior of a non-Newtonian fluid flow inside the space between two cylinders. The study investigated the effect of certain specific values of parameters such as inertia value with a range of Re (1, 10, 50) and the undulation number for the inner wall surface (n_u = 0, 6, 12, 24) numerically.

- It was found that an increase in the inertia parameter leads to a higher intensity of thermal buoyancy, thereby amplifying the heat transfer rate, especially at Re = 50.
- The dynamic behavior of the flow is also affected by increasing the Reynolds value, particularly at Re = 50. This increase disrupts the formation of stagnant regions, resulting in accelerated fluid flow
- The wavy cylinder shape with an undulation number of n_u= 24 demonstrated significantly higher thermal efficiency compared to the other cases examined. This particular configuration exhibited a notably higher Nusselt value (heat transfer rate).However For the hydrodynamics case, it was observed that the configuration with an undulation number of n_u = 6 proved to be more efficient in enhancing the flow of fluid within the system.
- The findings showed that increasing the inertia parameter and changing the geometry design of the examined geometry system altered the thermo-hydrodynamic structure between coaxial cylinders by accelerating the fluid flow field and increasing thermal heat transfer.
- Future research should encompass the exploration of alternative geometries and configurations to determine if the observed trends are consistent across different systems. Additionally, examining other complex fluids would further contribute to a more comprehensive understanding of flow patterns and heat transfer structures within these systems. These investigations are crucial for advancing our knowledge in the field of fluid dynamics and heat transfer, providing valuable insights for practical applications.

NOMENCLATURE

A	Area between two cyliders (m^2)
R	Radius of the outer cylinder (m)
r	Radius of inner cylinders (m)
N	Rotational speed (s-1)
n_u	Undulation numbers (-)
P	Pressure (Pa)
Pr	Prandtl number (-)
Re	Reynolds number (-)
Bn	Bingham number (-)
Tc	Cold temperature (K)
Th	Hot temperature (K)
u, v	Velocity components (m/s)
x, y	Cartesian directions (m)
Nu	Average Nusselt number (-)
Nul	Local Nusselt number (-)
m	The stress growth parameter (s)
M	Dimensionless stress parameters (-)
Y_P	Plasticity parameter (-)
x,y	Cartesian coordinates (*m*)
U,V	Dimensionless velocity (m)
X,Y	Dimensionless cartizian coordinate (-)
Vt	Tangential Velocity (-)

Greek symbols

ρ	Fluid density (kg •m−3)
α	Thermal diffusivity (m^2/s)
τ	Stress tensor, Pa
γ	Shear rate (1/s)
μ	Dynamic viscosity (Pa • s)
μ_p	Plastic viscosity (Pa.s)
ψ	Stream function (-)

AUTHORSHIP CONTRIBUTIONS

Authors equally contributed to this work.

DATA AVAILABILITY STATEMENT

The authors confirm that the data that supports the findings of this study are available within the article. Raw data that support the finding of this study are available from the corresponding author, upon reasonable request.

CONFLICT OF INTEREST

The author declared no potential conflicts of interest with respect to the research, authorship, and/or publication of this article.

ETHICS

There are no ethical issues with the publication of this manuscript.

REFERENCES

[1] Sonawane C, Praharaj P, Kulkarni A, Pandey A, Panchal H. Numerical simulation of heat transfer characteristics of circular cylinder forced to oscillate elliptically in an incompressible fluid flow. J Therm Anal Calorim. 2023;148:2719−2736. [CrossRef]

[2] Sonawane C, Praharaj P, Pandey A, Kulkarni A, Kotecha K, Panchal H. Case studies on simulations of flow-induced vibrations of a cooled circular cylinder: Incompressible flow solver for moving mesh problem. Case Stud Therm Eng. 2020;34:102030. [CrossRef]

[3] Leong JC, Lai FC. Mixed convection in a rotating concentric annulus with a porous sleeve. J Thermophys Heat Transf. 2019;33:483−494. [CrossRef]

[4] Hayat T, Khan M, Wang Y. Non-Newtonian flow between concentric cylinders. Commun Nonlinear Sci Numer Simul. 2006;11:297−305. [CrossRef]

[5] Kada B, Lakhdar R, Brahim M, Ameur H. Agitation of Complex Fluids in Cylindrical Vessels by Newly Designed Anchor Impellers. Period Polytech Mech Eng. 2022;1−11. [CrossRef]
[6] Behanifia K, Rahmani L, Brahim M, Al-Farhany K. Numerical investigation of laminar stirring viscous fluid inside stirred tank with newly Rushton turbine design. AIP Conference Proceedings. 2023;2787:090038. [CrossRef]
[7] Mehrizi AA, Farhadi M, Shayamehr S. Natural convection flow of Cu-Water nanofluid in horizontal cylindrical annuli with inner triangular cylinder using lattice Boltzmann method. Int Commun Heat Mass Transf. 2013;44:147−156. [CrossRef]
[8] Hadidi H, Manshadi MKD, Kamali R. Natural Convection of Power-Law Fluids Inside an Internally Finned Horizontal Annulus. Iran J Sci Technol - Trans Mech Eng. 2020;44:415−425. [CrossRef]
[9] Jalili P, Narimisa H, Jalili B, Ganji DD. Micro-polar nanofluid in the presence of thermophoresis, hall currents, and Brownian motion in a rotating system. Mod Phys Lett B. 2023;37:2250197. [CrossRef]
[10] Jalili P, Narimisa H, Jalili B, Shateri A, Ganji DD. A novel analytical approach to micro-polar nanofluid thermal analysis in the presence of thermophoresis, Brownian motion and Hall currents. Soft Comput. 2023;27:677−689. [CrossRef]
[11] Hussain A, Javed F, Nadeem S. Numerical Solution of a Casson Nanofluid flow and heat transfer analysis between Concentric Cylinders. 2019;99:25−30.
[12] Jalili B, Rezaeian A, Jalili P, Ommi F, Ganji DD. Numerical modeling of magnetic field impact on the thermal behavior of a microchannel heat sink. Case Stud Therm Eng. 2023;45:102944. [CrossRef]
[13] Brahim M, Benhanifia K, Jamshed W, Al-Farhany K, Redouane F, Eid MR, et al. Computational Analysis of Viscoplastic Nanofluid Blending by a Newly Modified Anchorage Impeller within a Stirred Container. Symmetry (Basel). 2022;14:2279. [CrossRef]
[14] Benhanifia K, Redouane F, Lakhdar R, Brahim M, Al-Farhany K, Jamshed W, et al. Investigation of mixing viscoplastic fluid with a modified anchor impeller inside a cylindrical stirred vessel using Casson-Papanastasiou model. Sci Rep. 2022;12:1−19. [CrossRef]
[15] Laidoudi H, Ameur H, Sahebi SAR, Hoseinzadeh S. Thermal Analysis of Steady Simulation of Free Convection from Concentric Elliptical Annuli of a Horizontal Arrangement. Arab J Sci Eng. 2022;47:15647−15660. [CrossRef]
[16] Rouhani F, Zakerzadeh MR, Baghani M. Pt Nu Sc Sc. 2018;1−4.
[17] Wu YH, Liu KF. Start-up flow of a Bingham fluid between two coaxial cylinders under a constant wall shear stress. J Nonnewton Fluid Mech. 2015;223(September):116−121. [CrossRef]
[18] Aboud ED, Rashid HK, Jassim HM, Ahmed SY, Khafaji SOW, Hamzah HK, et al. MHD effect on mixed convection of annulus circular enclosure filled with Non-Newtonian nanofluid. Heliyon. 2020;6:e03773. [CrossRef]
[19] Zerari K, Afrid M, Groulx D. Forced and mixed convection in the annulus between two horizontal confocal elliptical cylinders. Int J Therm Sci. 2013;74:126−144. [CrossRef]
[20] Soleimani M, Sadeghy K. Dean instability of bingham fluids in tangential flow between two fixed concentric cylinders. Nihon Reoroji Gakkaishi. 2010;38:125−132. [CrossRef]
[21] Khellaf K, Lauriat G. Numerical study of heat transfer in a non-Newtonian Carreau-fluid between rotating concentric vertical cylinders. J Nonnewton Fluid Mech. 2000;89:45−61. [CrossRef]
[22] Masoumi H, Aghighi MS, Ammar A, Nourbakhsh A. Laminar natural convection of yield stress fluids in annular spaces between concentric cylinders. Int J Heat Mass Transf. 2019;138:1188−1198. [CrossRef]
[23] Papanastasiou TC. Flows of materials with yield. J Rheol (N Y N Y). 1987;31:385−404. [CrossRef]
[24] Housiadas KD, Georgiou GC. The analytical solution for the flow of a Papanastasiou fluid in ducts with variable geometry. J Nonnewton Fluid Mech. 2023;105074. [CrossRef]
[25] Olayemi OA, Salaudeen A, Al-Farhany K, Medupin RO, Adegun IK. Modelling of heat transfer characteristics around a cylindrical-barrier. Int J Eng Model. 2022;35:83−106. [CrossRef]
[26] Marouche M, Anne-Archard D, Boisson HC. A numerical model of yield stress fluid dynamics in a mixing vessel. Appl Rheol. 2002;12:182−191. [CrossRef]